Available online at www.sciencedirect.com

ScienceDirect

Scripta Materialia 98 (2015) 32–35

Scripta MATERIALIA

www.elsevier.com/locate/scriptamat

Effects of oxygen on prismatic faults in α-Ti: a combined quantum mechanics/molecular mechanics study

M.A. Bhatia,[a] X. Zhang,[b] M. Azarnoush,[a] G. Lu[b] and K.N. Solanki[a,*]

[a] *School for Engineering of Matter, Transport, and Energy, Arizona State University, Tempe, AZ 85287, USA*
[b] *Department of Physics and Astronomy, California State University Northridge, Northridge, CA 91330, USA*

Received 7 October 2014; revised 5 November 2014; accepted 12 November 2014
Available online 29 November 2014

The mechanical properties of α-Ti are greatly affected by the presence of oxygen impurities. Here we focus on the interaction of oxygen with prismatic faults and oxygen diffusion barriers in α-Ti using a multiscale quantum mechanics/molecular mechanics approach. We show that a one-sixth monolayer of oxygen addition increases the Peierls stress 4-fold and reduces the dislocation core width by 18%. The calculated hardening effect due to oxygen and the oxygen diffusion barriers are consistent with experiments.

Keywords: Oxygen; Dislocation; First principles; Peierls stress

Titanium (Ti) and its alloys have been traditionally used for structural applications in automotive, aerospace and biomedical applications due to their high strength-to-weight ratios [1]. Commercially pure Ti alloys are particularly attractive due to their excellent corrosion resistance, light weight and formability. Crucial to the mechanical properties of these alloys is the presence of oxygen impurities. Specifically, it has been shown that the oxygen impurities can either harden or soften the materials as a result of the interaction between the impurities and lattice defects, particularly dislocations and twins [2–4]. In high strength grade Ti alloys the addition of oxygen improves the corrosion and wear resistance of α-Ti and its alloys [1,5]. However, at elevated temperatures an oxide layer at the Ti surface is formed and the O atoms can diffuse rapidly into the base metal [4], instigating hardening and embrittlement of the base material [3]. In particular, a dislocation core could act as a fast path for diffusing O atoms whose mobility can be orders of magnitude higher than those in bulk diffusion; this phenomenon is often referred to as "pipe diffusion". By creating a short-circuit pathway the pipe diffusion can affect many kinetic processes in the bulk materials, including creep [6], dynamic-strain aging, crystallization [7], and other mechanical properties of α-Ti. Consequently, understanding the atomistic mechanisms behind oxygen–metal interaction is crucial for developing high-performance Ti alloys [2,8,9] with applications in nuclear power plants, wind turbines and other large-scale industrial infrastructure.

In this paper we examine oxygen diffusion in bulk α-Ti and pipe diffusion along a prismatic edge dislocation core. In addition, we evaluate the dislocation mobility in the presence and absence of oxygen impurities. We have employed a coupled quantum mechanics and molecular mechanics (QM/MM) method that combines the accuracy of QM calculations with the simplicity and efficiency of MM simulations. In conjunction with a climb-based nudged elastic band (C-NEB) method [10] we can determine the oxygen diffusion barriers accurately. More specifically, the QM/MM model is partitioned into two spatial domains: a QM region consisting of the dislocation core and the oxygen impurity, and an MM region for the rest of the system. In the QM region the energy and force are calculated based on the density functional theory (DFT) [11,12] as implemented in the Vienna Ab initio Simulation Package (VASP) [13], while the same quantities in the MM region are computed by empirical atomistic simulations [14] based on the embedded atom method (EAM) due to Zope and Mishin [15] (see the online Supplementary Information). The coupling between the QM and MM regions is accomplished by the constrained DFT [16]. The post-processing of the simulation data is performed using OVITO [17]. Complementary to the atomistic simulations, the semi-discrete variational Peierls–Nabarro model (SVPN) [18] was also used to analyze the dislocation core structure and mobility. The chemical interaction between the oxygen impurity and the dislocation core is captured by the so-called generalized stacking fault energy (GSFE) surface which was determined from DFT-VASP calculations. By

* Corresponding author. Tel.: +1 (480)965 1869; fax: +1 (480)727 9321; e-mail: kiran.solanki@asu.edu

http://dx.doi.org/10.1016/j.scriptamat.2014.11.008
1359-6462/

taking the chemical interaction into consideration the SVPN model can predict the dislocation core structure and mobility in the presence and absence of the oxygen impurity and thus reveal the effect of oxygen on the softening/hardening behavior in α-Ti.

An edge dislocation was created, as described by Osetsky and Bacon [19], initially in LAMMPS [20]. The edge dislocation structure obtained using the EAM potential was further relaxed using the QM/MM method with 30 meV Å^{-1} and 1 meV as the force and energy convergence criterion, respectively. The QM region had 196 atoms containing the dislocation core with/without an oxygen impurity and the MM region consisted of 11,926 atoms capturing the long-range elastic field of the dislocation. The overall dimensions of different regions were: 30 Å × 27 Å × 9.26 Å for the QM region, and 143.67 Å × 155.07 Å × 9.26 Å for the MM region. The simulations were performed on a rectangular cell having x, y and z axes oriented along the $[1\bar{2}10], [10\bar{1}0]and[0001]$ directions, respectively. The length along the dislocation line [0001] was set to $2c$ ($c = 4.645$ Å) to avoid the interaction of O atoms due to periodic boundary conditions.

For the DFT part, projector augmented wave (PAW) [21] potentials were used to represent the nuclei core with valence electrons on s and d orbitals for α-Ti and valence electrons on s and p orbitals for O atoms. Exchange and correlation was treated with GGA using the PBE [22] form with an energy cutoff of 289 eV and a Monkhorst–Pack k-point mesh of $1 \times 1 \times 5$ along the $[1\bar{2}10], [10\bar{1}0]$ and [0001] respectively. For GSFE calculations the k-point mesh was $18 \times 1 \times 10$ along the $[1\bar{2}10], [10\bar{1}0]$ and [0001] respectively. A single O atom was introduced on the prismatic shearing plane with 1/6 monolayer (ML) oxygen concentration; the slip direction is along $[1\bar{2}10]$. The O atom was free to relax in all directions, whereas Ti atoms were free to move along the $[10\bar{1}0]$ direction only.

First we focus on oxygen diffusion in bulk α-Ti. There are three interstitial positions, octahedral, crowdion and hexahedral sites, which the O may occupy, and the preferred position is the octahedral site [8]. The hexahedral site is on the basal plane, whereas the octahedral and crowdion sites are between the A and B stacking along the [0001] direction [8]. The transition pathways and energy barriers between the different interstitial sites for a diffusing O atom have been determined using the C-NEB method with four intermediate images. Figure 1 shows the energy barriers for the O atom diffusing from an octahedral site to an adjacent crowdion site (O—C) and subsequently from a crowdion position to a hexahedral position (C—H) and finally from a hexahedral position to an octahedral position (H—O). Also in Figure 1, the diffusion pathway is illustrated by showing the O positions along the transition path. The potential energy of the hexahedral site is 1.43 eV higher than that of the octahedral site. Moreover the excess energy of the crowdion site over the octahedral site is 1.95 eV. Both crowdion and hexahedral sites are local energy minima and thus excess thermal energy is required for the O atom to reach the octahedral sites. The diffusion energy barriers from the crowdion and the hexahedral sites to the octahedral sites are 120 and ~550 meV, respectively. Both compare well with the work of Wu and Trinkle [8].

Next we study oxygen–dislocation interaction in α-Ti. To this end we first need to determine the relative site preference of oxygen at the dislocation core. The total energy of a single O atom placed at various interstitial sites near and away from the dislocation core has been calculated. Figure 2a shows the optimized equilibrium geometry of the oxygen at the prismatic edge dislocation in α-Ti viewed along the [0001] direction. It is found that the local atomic configuration changes from a hexagonal close-packed (hcp) octahedral to a body-centered cubic (bcc) octahedral structure. The O atom binds with four Ti atoms on the same basal plane and with two Ti atoms above and below the plane. The O position is the same as in the hexahedral site in bulk α-Ti except that now there are four atoms on the basal plane (see Fig. 2b) instead of three (Fig. 1).

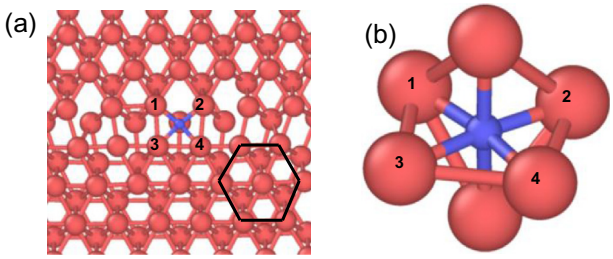

Figure 2. (a) Oxygen binding at the prismatic dislocation core with the plane of sight along the [0001] direction. (b) Oxygen binds with six Ti atoms at the dislocation core. Atoms are marked by numbers on the basal plane.

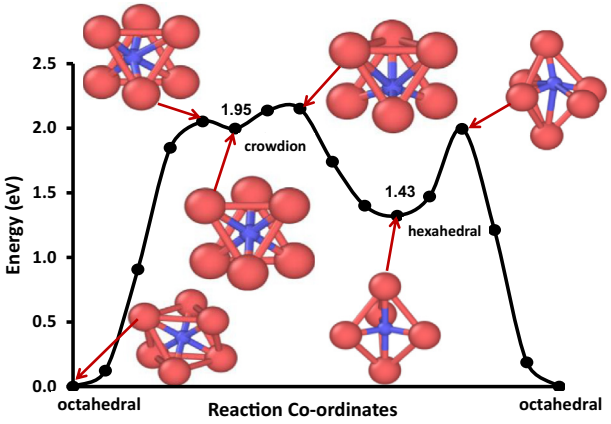

Figure 1. C-NEB path and energy barriers for an O atom diffusing in bulk α-Ti between the interstitial sites.

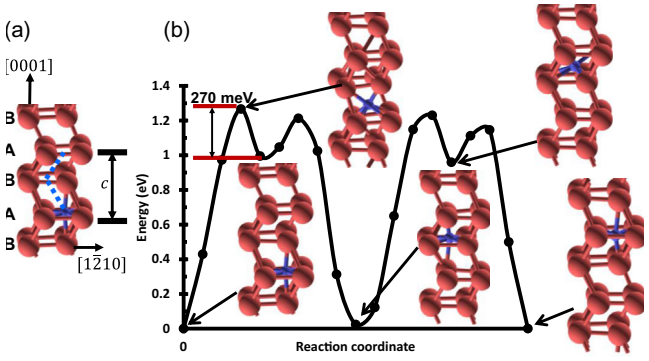

Figure 3. (a) Diffusion path of an O atom along the dislocation line ([0001] direction) of the prismatic edge dislocation with ABAB stacking sequence. (b) The C-NEB path for an O atom diffusing along the dislocation line.

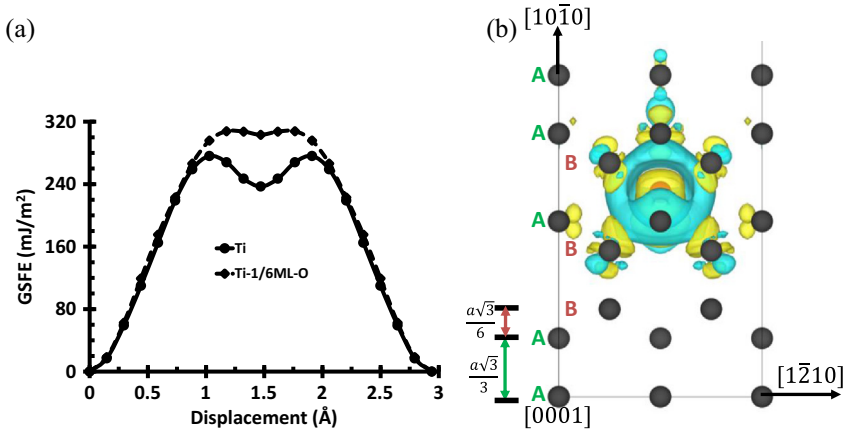

Figure 4. (a) GSFE as a function of shear displacement along the [1$\bar{2}$10] direction of α-Ti with and without 1/6 ML oxygen on the slip plane. (b) A 3-D isosurface plot for charge density showing the effect of O at the prismatic stacking fault. The orange and black atoms represent O and Ti atoms, respectively. The yellow and cyan isosurfaces represent charge accumulation and depletion, respectively. (For interpretation of color in Figure 4, the reader is referred to the web version of this article.)

Having obtained the stable oxygen site at the dislocation core, we proceed to determine the oxygen diffusion pathway and energy barriers along the dislocation core using the C-NEB method with 16 intermediate images. Figure 3a shows the initial path for an O atom to diffuse over a distance of c (4.645 Å) in the dislocation line direction of [0001] with ABAB stacking. The energy barrier and diffusion path for the pipe diffusion of O along the dislocation line are depicted in Figure 3b. Also the migration pathway is illustrated by showing the O position along the path in Figure 3b. The energy barrier for the diffusion path from one bcc octahedral position to another bcc octahedral position is 1.24 eV, which is much smaller than the bulk diffusion barrier of 2.0 eV. To put the results in perspective we can estimate the required temperature for an O atom jumping from one octahedral site to the next in the bulk α-Ti and for the pipe diffusion along the dislocation line. Assuming the phonon frequency as 10^{13} s^{-1} and for a unit probability, the required temperature for the bulk diffusion is 775 K, much higher than that of the pipe diffusion at 496 K.

Next we examine the effect of oxygen on the deformation behavior α-Ti using the SVPN model in conjunction with the ab initio determined GSFE. Figure 4a illustrates the GSFE curves as a function of the shear displacement in the [1$\bar{2}$10] direction with (the oxygen concentration is 1/6 ML) and without the interstitial oxygen. The unstable stacking fault energy is increased from 237 to 303 mJ m^{-2} (28% increase) in the presence of oxygen on the shear plane. The dislocation core width and the Peierls stress were calculated using the SVPN method with ab initio GSFE. The Peierls stress for the prismatic edge dislocation with and without oxygen was found to be 97 and 24 MPa, respectively (~400% increase). The simulations also revealed that the prismatic dislocation becomes narrower in the presence of oxygen, from 1.1 to 0.9 Å. This narrowing of the core width is consistent with the increase of the Peierls stress since the Peierls stress depends exponentially on the ratio between the dislocation core width and the atomic spacing along the dislocation line.

The mechanical properties of a material are determined by the nature of atomic bonding; therein, both the shear strength and cohesive energy are affected by the directionality and strength of chemical bonds. Therefore, understanding the change in charge density resulting from a solute atom can shed light on the strengthening mechanism of the impurity [23]. Figure 4b presents a 3-D isosurface plot for the differential charge density in the presence of the O atom. The yellow and cyan isosurfaces represent charge accumulation and depletion, respectively. Compared to the charge density distribution in pure α-Ti the main change due to oxygen happens around the octahedral site as seen in Figure 4b. The charge densities between Ti atoms were evidently increased, with the addition of oxygen resulting in an increase in the shear modulus which affects the dislocation mobility.

In summary, the oxygen–metal interaction in α-Ti was examined including oxygen diffusion barriers and oxygen effects on the prismatic edge dislocation ($\{10\bar{1}0\}\langle 1\bar{2}10\rangle$) motion. It was found that oxygen prefers to occupy the bcc octahedral site at the dislocation core. Moreover, the oxygen diffusion barrier along the edge dislocation line from a bcc octahedral position to an hcp octahedral position is 1.24 eV, which is much smaller than the bulk diffusion barrier of 2.0 eV. We show that a one-sixth ML of oxygen addition increases the Peierls stress 4-fold and reduces the dislocation core width by 18%. The charge densities between Ti atoms were increased with the addition of oxygen at the prismatic fault resulting in an increase in the shear modulus. The calculated hardening effect of oxygen and oxygen diffusion barriers are consistent with those experimentally observed [3]. Overall our study provides critical knowledge towards a comprehensive understanding of the effects of oxygen on the deformation behaviors of α-Ti.

The authors gratefully acknowledge support from the Air Force Office of Scientific Research under contract FA9550-13-1-0144. The work at California State University Northridge was supported by the Office of Naval Research.

Supplementary data associated with this article can be found, in the online version, at http://dx.doi.org/10.1016/j.scriptamat.2014.11.008.

[1] C. Leyens, M. Peters, Titanium and titanium alloys: fundamentals and applications, 2003.
[2] M.C. Brandes, M. Baughman, M.J. Mills, J.C. Williams, Mater. Sci. Eng. A 551 (2012) 13.

[3] H. Dong, X.Y. Li, Mater. Sci. Eng. A 280 (2000) 303.
[4] Z. Liu, G. Welsch, Metall. Trans. A 19 (1988) 1121.
[5] J. Stringer, Acta Metall. 8 (1960) 758.
[6] A.B. Pandey, R.S. Mishra, A.G. Paradkar, Y.R. Mahajan, Acta Mater. 45 (1997) 1297.
[7] W. Luo, C. Shen, Y. Wang, Acta Mater. 55 (2007) 2579.
[8] H.H. Wu, D.R. Trinkle, Phys. Rev. Lett. 107 (2011) 045504.
[9] J.C. Williams, A.W. Sommer, P.P. Tung, Metall. Trans. 3 (1972) 2979.
[10] G. Henkelman, B.P. Uberuaga, H. Jónsson, J. Chem. Phys. 113 (2000) 9901.
[11] Q. Zhao, R.G. Parr, J. Chem. Phys. 98 (1993) 543.
[12] Q. Zhao, R.C. Morrison, R.G. Parr, Phys. Rev. A 50 (1994) 2138.
[13] G. Kresse, J. Hafner, Phys. Rev. B 47 (1993) 558.
[14] M.S. Daw, M.I. Baskes, Phys. Rev. Lett. 50 (1983) 1285.
[15] R.R. Zope, Y. Mishin, Phys. Rev. B 68 (2003) 024102.
[16] X. Zhang, G. Lu, W.A. Curtin, Phys. Rev. B 87 (2013) 054113.
[17] A. Stukowski, Model. Simul. Mater. Sci. Eng. 18 (2010) 015012.
[18] V.V. Bulatov, E. Kaxiras, Phys. Rev. Lett. 78 (1997) 4221.
[19] Y.N. Osetsky, D.J. Bacon, Model. Simul. Mater. Sci. Eng. 11 (2003) 427.
[20] S. Plimpton, J. Comput. Phys. 117 (1995) 1.
[21] P.E. Blöchl, Phys. Rev. B 50 (1994) 17953.
[22] J.P. Perdew, K. Burke, M. Ernzerhof, Phys. Rev. Lett. 78 (1997) 1396.
[23] Y. Song, Z. Guo, R. Yang, Philos. Mag. A 82 (2002) 1345.